

## ARTICLE



# Targeting PDK2 rescues stress-induced impaired brain energy metabolism

Changshui Wang<sup>1,5</sup>, Changmeng Cui<sup>1,5</sup>, Pengfei Xu<sup>2</sup>, Li Zhu<sup>2</sup>, Hongjia Xue<sup>3</sup>, Beibei Chen<sup>4</sup> and Pei Jiang<sup>2</sup>✉

© The Author(s), under exclusive licence to Springer Nature Limited 2023

Depression is a mental illness frequently accompanied by disordered energy metabolism. A dysregulated hypothalamus pituitary adrenal axis response with aberrant glucocorticoids (GCs) release is often observed in patients with depression. However, the associated etiology between GCs and brain energy metabolism remains poorly understood. Here, using metabolomic analysis, we showed that the tricarboxylic acid (TCA) cycle was inhibited in chronic social defeat stress (CSDS)-exposed mice and patients with first-episode depression. Decreased mitochondrial oxidative phosphorylation was concomitant with the impairment of the TCA cycle. In parallel, the activity of pyruvate dehydrogenase (PDH), the gatekeeper of mitochondrial TCA flux, was suppressed, which is associated with the CSDS-induced neuronal pyruvate dehydrogenase kinase 2 (PDK2) expression and consequently enhanced PDH phosphorylation. Considering the well-acknowledged role of GCs in energy metabolism, we further demonstrated that glucocorticoid receptors (GR) stimulated PDK2 expression by directly binding to its promoter region. Meanwhile, silencing PDK2 abrogated glucocorticoid-induced PDH inhibition, restored the neuronal oxidative phosphorylation, and improved the flux of isotope-labeled carbon (U-<sup>13</sup>C) glucose into the TCA cycle. Additionally, in vivo, pharmacological inhibition and neuron-specific silencing of GR or PDK2 restored CSDS-induced PDH phosphorylation and exerted antidepressant activities against chronic stress exposure. Taken together, our findings reveal a novel mechanism of depression manifestation, whereby elevated GCs levels regulate PDK2 transcription via GR, thereby impairing brain energy metabolism and contributing to the onset of this condition.

*Molecular Psychiatry*; <https://doi.org/10.1038/s41380-023-02098-9>

## INTRODUCTION

Major depressive disorder (MDD) is one of the most common and debilitating mental illnesses and a serious health challenge for society [1]. Individuals can develop depression after going through stressful or traumatic events. The clinical symptoms of MDD include anhedonia, fatigue, poor memory, and lack of motivation, effects that have been linked to reduced brain activity [2, 3]. The brain is among the most metabolically active organs in the human body and is dependent on a continuous supply of energy to maintain normal function [4, 5]. Brain energy metabolism disorder has been widely implicated in psychiatric diseases, including depression [6–8].

The human brain only makes up 2% of the body mass but utilizes 25% of the total glucose consumption in the body [9]. Normally, glucose is the primary energy source for the brain and is metabolized into adenosine triphosphate (ATP) via glycolysis, the tricarboxylic acid (TCA) cycle and the electron transport chain [10]. Glycolysis is a metabolic process in the cytosol that breaks down glucose into pyruvate in the cytosol. Pyruvate enters the mitochondria and converted to acetyl coenzyme A (acetyl-CoA) by the pyruvate dehydrogenase (PDH), which is phosphorylated and inactivated by pyruvate dehydrogenase kinases (PDK) [11]. Subsequently, acetyl-CoA enters the TCA cycle, producing NADH

and FADH<sub>2</sub>, which are then transported to the electron transport chain and generate a transmembrane proton gradient across the inner mitochondrial membrane, generating ATP and providing energy for cells [12]. Impaired brain glucose metabolism leads to decreased NADPH levels and impaired redox balance and ATP production in mitochondria [13, 14].

Glucocorticoids (GCs), steroid hormones, function as crucial regulators of energy metabolism and immune responses, and impaired glucocorticoid signaling is thought to be a leading cause of depression [15–18]. Long-term stress induces hypothalamic pituitary adrenal (HPA) axis dysregulation, which leads to the release of GCs from the adrenal cortex [19]. GCs can cross the blood-brain barrier and diffuse into the brain, where they bind to glucocorticoid receptors (GR) [20], which triggers their translocation into the nucleus and their binding to glucocorticoid response elements (GREs) in the promoters of target genes [21]. GCs mediate glucose homeostasis in the liver and decrease glucose utilization in muscles by binding to the GR [22, 23]. Several studies have shown that excessive high glucocorticoid concentrations can suppress brain glucose utilization [24]. PDH, a rate-limiting enzyme for glucose metabolism, is a key link between glycolysis and the TCA cycle [25]. PDH activity is tightly regulated by PDK. Among the four known PDK isoforms, PDK2 is the most widely distributed [26, 27]. The

<sup>1</sup>Department of Neurosurgery, Affiliated Hospital of Jining Medical University, Jining Medical University, Jining 272000, China. <sup>2</sup>Translational Pharmaceutical Laboratory, Jining First People's Hospital, Shandong First Medical University, Jining 272000, China. <sup>3</sup>Faculty of Science and Engineering, University of Nottingham Ningbo China, Ningbo 315100, China. <sup>4</sup>ADFA School of Science, University of New South Wales, Canberra, ACT, Australia. <sup>5</sup>These authors contributed equally: Changshui Wang, Changmeng Cui.

✉email: [jiangpeicsu@sina.com](mailto:jiangpeicsu@sina.com)

Received: 16 April 2022 Revised: 27 April 2023 Accepted: 28 April 2023

Published online: 15 May 2023

expression and kinetic activity of PDK is regulated by nuclear hormone receptors such as GR, peroxisome proliferator-activated receptors, and estrogen-related receptors [28].

Although the mechanisms of underlying depression pathogenesis remain poorly understood, increasing evidence suggests that brain energy metabolism dysfunction is linked with the pathogenesis of this condition. Here, we show that stress decreases the levels of TCA cycle intermediates, implying that the TCA cycle is impaired. Importantly, we found that the GCs bind to the GR, which binds to the GREs in the PDK2 promoter and induce its transcription, thereby suppressing PDH enzymatic activity and leading to metabolite flux dysfunction. We also found that PDK2 silencing improves chronic social defeat stress (CSDS)-induced depression-like behavior in mice.

## MATERIALS AND METHODS

In this study, 41 first-episode MDD patients and 49 sex-matched healthy controls were selected and included (Supplementary Table 1). Subject inclusion/exclusion criteria, animals, primary cortical neurons and astrocytes culture, chronic social defeat stress, behavioral test, metabolite extraction and analysis, GC-MS analysis, Multivariate Analysis of metabolic data, biochemical analysis, PDH activity analysis, gene silencing and overexpression experiments, oxygen consumption rate, measurement of mitochondrial membrane potential, chromatin immunoprecipitation assay, adeno-associated viral vector preparation and injection, western blot analysis, histopathology and immunofluorescence, Nissl staining, qRT-PCR analysis and statistical analysis are described in detail in the Supplementary Information.

## RESULTS

### Energy metabolism is disturbed in CSDS mice

It's widely accepted the social stress is the leading cause of depressive disorder in human [29]. Social avoidance, anhedonia and despair are the core symptoms of depression [30]. CSDS model is widely used to induce social avoidance and anhedonia, and considered as be the most representative animal model of depression [31]. Following the 10-day CSDS exposure, a series of tests assessing depression-like behavior was conducted (Fig. 1a). Typically, mice without CSDS spend an increased amount of time in the interaction zone when a target mouse is present. However, defeated mice tend to stay in the corners to avoid the aggressor and spend less time in social interaction with target mice [32]. Social interaction (SI) ratio was calculated based on the duration of interaction zone time with or without a target mouse present and 12 susceptible mice ( $SI < 1$ ) randomly selected as CSDS group and an equal number of mice not subjected to CSDS were selected as the control (CTRL) group. (Fig. 1b). Compared with control mice, susceptible mice displayed a significant increase in immobility time in the forced swim test (FST) after exposure to stress (Fig. 1c), which was accompanied by a reduction in the preference for sucrose in the sucrose preference test (SPT) (Fig. 1d). In the elevated plus maze (EPM) test, mice in the CSDS group spent significantly less time in the open arms and had significantly fewer entries in the open arms (Fig. 1e). The cortex plays a pivotal role in mediating stress-induced behavioral disorders, including MDD [33]. We identified potential differentially expressed metabolites in the frontal cortex and serum of mice and in the serum of first-episode MDD patients via metabolomics profiling. Orthogonal partial least squares discriminant analysis (OPLS-DA) showed the separation between both CTRL and CSDS mice and Control and MDD subjects (Fig. 1f-h). Additionally, a 200 times random permutation test was conducted, and the R2 and Q2 values confirmed the appropriateness of subsequent optimization analyses (Fig. 1i-k). In permutation test, the R2 and Q2 scores indicate the model's goodness of fit and predictive ability. Based on two criteria ( $VIP > 1$  and  $P$ -value  $< 0.05$ ), differentially abundant metabolites were identified in the cortex (Supplementary Fig. 1) and serum (Supplementary Fig. 2) of mice as

well as in the serum of depressed patients (Supplementary Fig. 3), while some of the TCA cycle-associated metabolites showed decreased levels. Pathway analysis also indicated a significant enrichment of metabolites in the TCA cycle pathway both in the CSDS model mice and in patients (Fig. 1l-n), implying a significant impairment of the TCA cycle.

To characterize the changes in brain metabolism occurring in CSDS mice, we further detected the content of several substrates relevant to glucose oxidation in different brain regions. Levels of acetyl-CoA, citric acid, and ATP were lower in the cortex of CSDS mice than in the cortex of CTRL mice (Fig. 2a, b). In the hippocampus, citric acid and ATP contents were significantly lower in the CSDS group than in the CTRL group; however, acetyl-CoA content showed no significant difference between the two groups (Supplementary Fig. 4a, b). The hypothalamus showed no difference in acetyl-CoA, citric acid, and ATP levels between the two groups (Supplementary Fig. 4c, d).

### Chronic stress enhances PDK2 expression and PDH phosphorylation

Given that PDH is a key regulator of the rate of entry of pyruvate into the TCA cycle for subsequent oxidation (Fig. 2c), we examined PDH activity and analyzed the correlation between PDH activity and SI ratio in the frontal cortex, hippocampus and hypothalamus. PDH enzymatic activity was significantly reduced in the cortex of CSDS mice, which was positively correlated with SI ratio (Fig. 2d, e). Additionally, in the hippocampus, PDH activity was significantly reduced in the CSDS mouse, but no correlation was detected between PDH activity and SI ratio (Supplementary Fig. 4e, f). In the hypothalamus, exposure to CSDS did not affect PDH activity and no correlation was found between PDH activity and SI ratio (Supplementary Fig. 4g, h). Next, we examined the levels of PDK isoforms at the mRNA level in the frontal cortex, hippocampus, and hypothalamus of CTRL and CSDS mice after exposure to stress. The results showed that mRNA levels of PDK2, but not PDK1, PDK3, and PDK4, were significantly higher in these three brain regions of CSDS mice than in the CTRL counterparts, and a significant negative correlation between PDK2 mRNA level and SI ratio was detected only in the cortex (Supplementary Fig. 4i-n). In addition, we further investigated the PDK mRNA levels and PDH activity in thalamus, amygdala, and ventral tegmental area (VTA). Among these sites, only the amygdala displayed a significant upregulation of PDK2 expression, whereas no significant differences in PDH activity were detected between CTRL and CSDS mice (Supplementary Fig. 5a-f). Considering that both PDK2 expression and PDH activity were significantly increased in the cortex, western blotting was then performed to verify the levels of PDK2 and phosphorylated PDH. The protein level of PDK2 was also significantly higher in the frontal cortex of CSDS mice (Fig. 2f), which led to a significant increase in PDH phosphorylation levels (p-PDH-S300 and p-PDH-S293) (Fig. 2f, Supplementary Fig. 5g, h). Immunofluorescence staining results further showed that PDK2 was mainly expressed in the neurons and astrocytes with negligible expression in microglia (Fig. 2g-i). Our *in vitro* findings also demonstrated that PDK2 was highly expressed both in the neurons and astrocytes (Supplementary Fig. 6a-d). However, CSDS exposure more pronouncedly induced neuronal PDK2 expression, and slightly but significantly induced PDK2 in astrocytes (Fig. 2g-i). We also compared the mRNA levels of PDK2 in the peripheral blood mononuclear cells of first-episode MDD patients and healthy controls. The PDK2 mRNA levels were higher in depressed patients than in healthy controls, and were significantly and positively associated with the Hamilton depression rating scale score (Fig. 2j, k).

### GR regulates PDK2 expression by binding to its promoter region

GCs are important regulators of energy metabolism and stress response [34]. Serum cortisol and corticosterone (CORT) contents

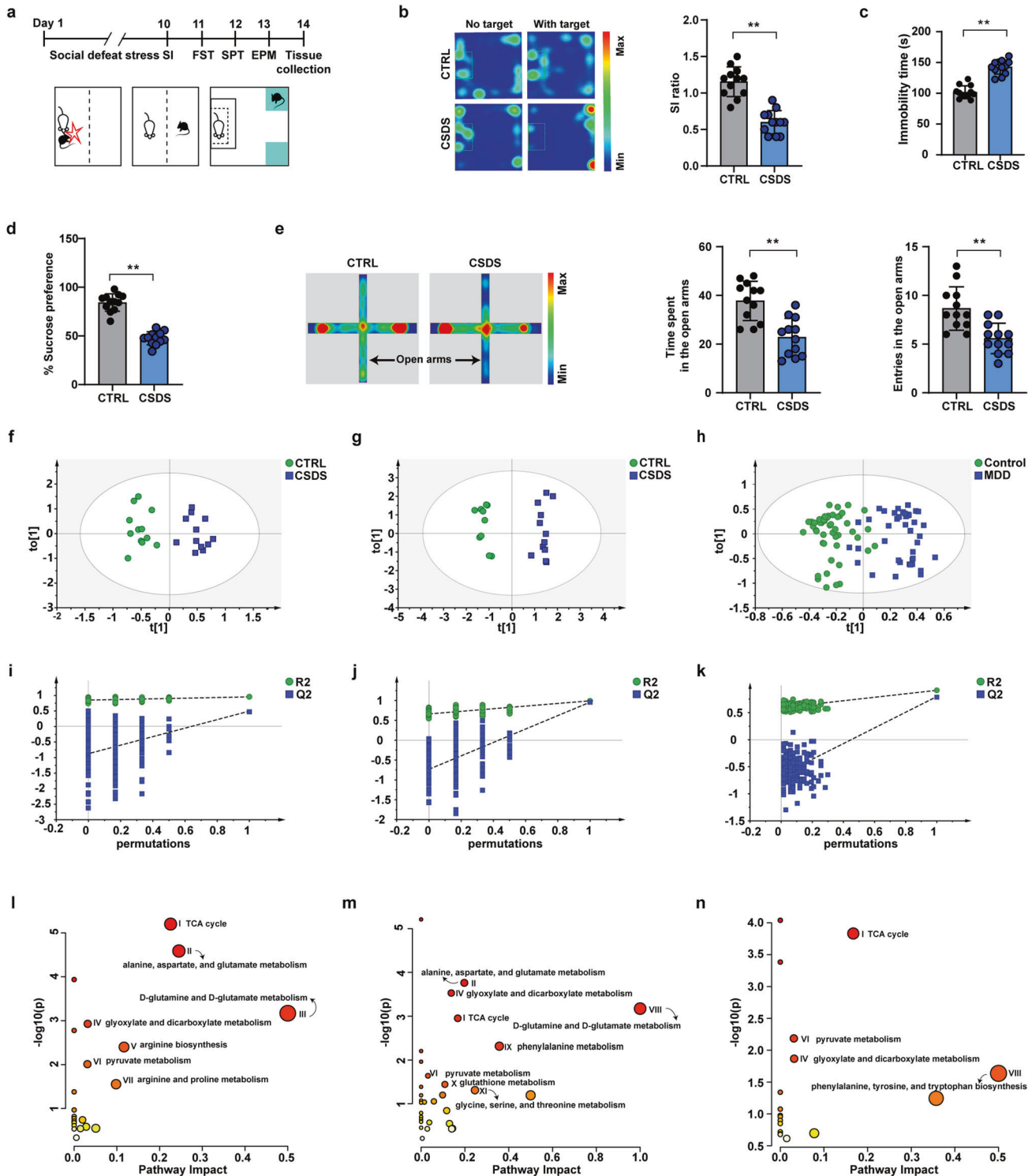


**Fig. 1** CSDS induced depression-like behaviors in mice, and metabolic profile of CSDS mice and first-episode MDD patients. **a** Experimental timeline of the CSDS and behaviour tests. The mice were subjected to 10-day consecutive social defeat by CD-1 aggressor, followed by SI, FST, SPT, and EPM test. **b** (Left) Heatmap of the trajectory of mice and (Right) statistical graph of SI ratio for CTRL and susceptible mice after CSDS exposure.  $n = 12$ ; unpaired Student's  $t$ -test. **c**, **d** CSDS increased the immobility time in the FST and decreased sucrose consumption in SPT.  $n = 12$ ; unpaired Student's  $t$ -test. **e** (Left) Heatmap of the trajectory of mice and (Right) CSDS decreased time spent in the open arms and number of entries into the open arms of the EPM test.  $n = 12$ ; unpaired Student's  $t$ -test. **f–h** OPLS-DA score plots of metabolic profiling in the mouse cortex, mouse serum, and serum from MDD patients. The 200 times permutation testing of OPLS-DA models in the mouse cortex (**i**), mouse serum (**j**), and serum from MDD patients (**k**). **l–n** MetaboAnalyst 5.0 summary of the pathway analysis of the mouse cortex, mouse serum, and serum from MDD patients.  $^{**}P < 0.01$ ; All data represent mean  $\pm$  SEM.

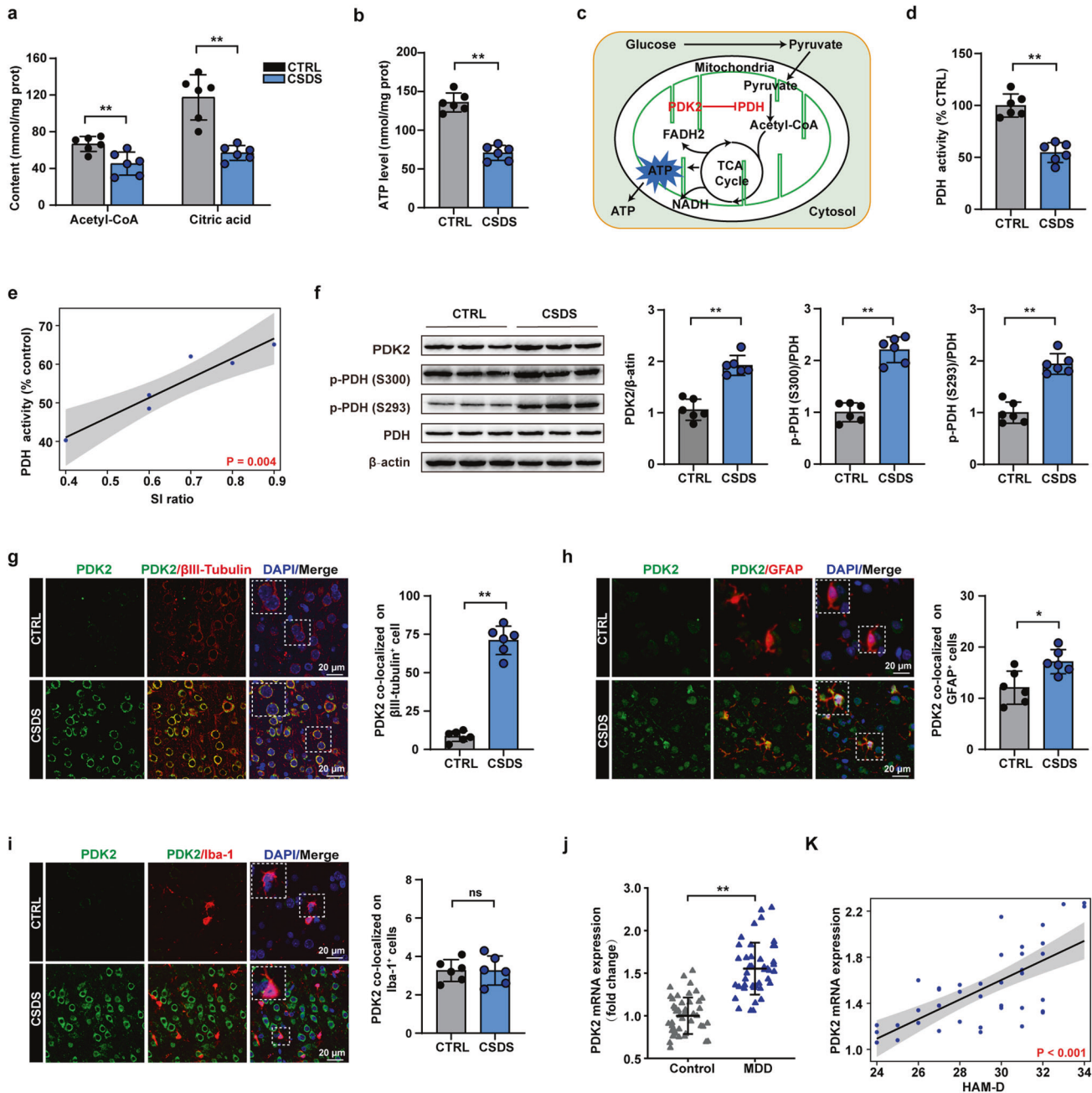
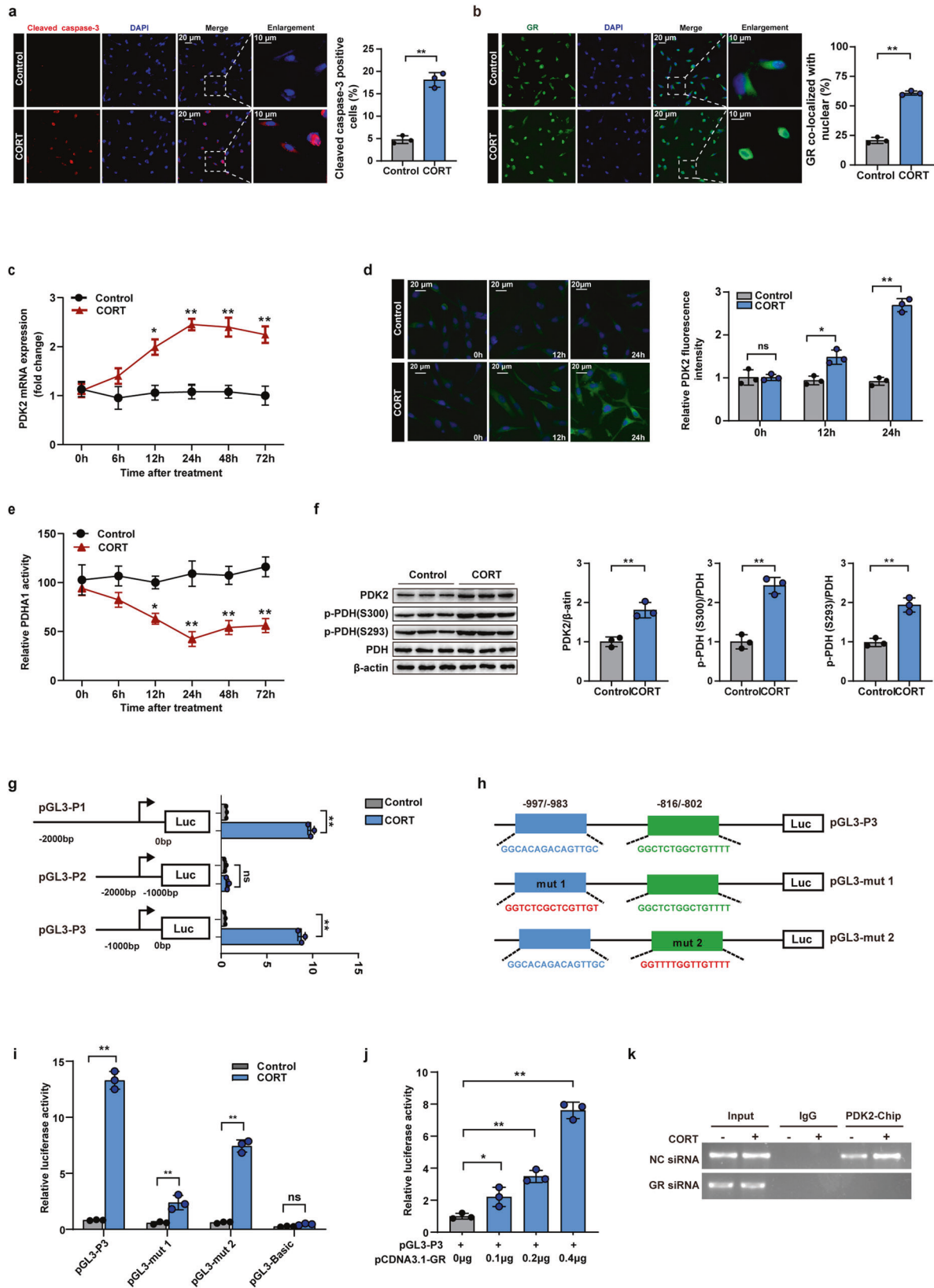


**Fig. 2** Expression of PDK and phosphorylated PDH in the mouse cortex following CSDS exposure. **a** CSDS decreased acetyl-CoA and citric acid content in cortex compared with CTRL mice.  $n = 6$ ; unpaired Student's *t*-test. **b** CSDS decreased ATP level in cortex compared with CTRL mice.  $n = 6$ ; unpaired Student's *t*-test. **c** A schematic illustrating the mechanism of the PDK-PDH axis regulating glycolysis and the TCA cycle. **d** CSDS decreased PDH activity in cortex.  $n = 6$ ; unpaired Student's *t*-test. **e** Correlation between PDH activity and SI ratio. Pearson's correlation coefficient. **f** The effect of CSDS on PDK2, phosphorylated PDH, and unphosphorylated PDH proteins levels in the cortex.  $n = 6$ ; unpaired Student's *t*-test. **g–i** Immunofluorescence co-staining of PDK2 with  $\beta$ III-tubulin, GFAP, and Iba-1 in the cortex after CSDS.  $n = 6$ ; unpaired Student's *t*-test. **j** Relative PDK2 expression level in the peripheral blood of MDD patients.  $n = 41$  first-episode MDD patients and 49 healthy individuals; unpaired Student's *t*-test. **k** Correlation between HAM-D scores and PDK2 expression in the peripheral blood of MDD patients. Pearson's correlation coefficient. ns=not significant, \* $P < 0.05$ , \*\* $P < 0.01$ ; All data represent mean  $\pm$  SEM.

were significantly increased in MDD patients and CSDS mice, respectively (Supplementary Fig. 7a, b). We further assessed the effect of CORT on neuron apoptosis and GR transport. The results showed that CORT treatment significantly increased the expression of cleaved caspase-3 (Fig. 3a). CORT-treated neurons induced an increase in the expression of GR and led to GR translocation to the nucleus (Fig. 3b), while mifepristone (RU486) pre-treatment prevented CORT from inducing GR expression and GR translocation to the nucleus (Supplementary Fig. 8a, b). We then examined

the effect of CORT exposure on PDK expression and PDH activity in neurons at different time points in vitro. The qRT-PCR results showed that PDK2 expression was significantly increased after 12 h of CORT exposure, and peaked at 24 h (Fig. 3c). No differences in PDK1, PDK3, or PDK4 expression were detected at any time point (Supplementary Fig. 8c–e). Consistent with the results of qRT-PCR, immunofluorescent staining showed that the level of PDK2 increased at 12 and 24 h (Fig. 3d). PDH activity was inhibited by the high level of PDK2 mRNA (Fig. 3e). Similarly, the



protein level of PDK2 and the p-PDH/PDH ratio were both increased in primary cortical neurons after CORT exposure (Fig. 3f). Collectively, these data indicated that CORT exposure led to an increase in PDK2 expression and the suppression of PDH activity.

GCs regulate gene transcription by activating the GR, which then binds to GREs in the promoter regions of target genes [35]. To determine if the GR mediates CORT-dependent induction of PDK2 expression, we cloned three PDK2 promoter fragments of different

**Fig. 3 GR regulates PDK2 gene expression by binding to its promoter. a, b** Effect of CORT on the expression of cleaved caspase-3 and GR as detected by immunofluorescence. **c, d** Expression analysis of PDK2 at the indicated time points after CORT treatment by qRT-PCR and immunofluorescence.  $n = 3$ ; two-way ANOVA. **e** The effect of CORT on PDH activity was analyzed at the indicated time points.  $n = 3$ ; two-way ANOVA. **f** The effect of CORT on PDK2, phosphorylated PDH, and unphosphorylated PDH proteins levels in primary cortical neurons cells.  $n = 3$ ; unpaired Student's *t*-test. **g** Luciferase activity in different segments of the PDK2 promoter with or without CORT treatment.  $n = 3$ ; unpaired Student's *t*-test. **h** Schematic diagram of potential GR binding sites in the PDK2 promoter, and schematic of site-directed mutagenesis of the PDK2 promoter. **i** Luciferase activity of site-directed mutagenesis in primary cortical neurons with or without CORT treatment.  $n = 3$ ; unpaired Student's *t*-test. **j** Dose-dependent effect of GR overexpression on luciferase activity.  $n = 3$ ; two-way ANOVA. **k** ChIP-PCR assay showing the binding of GR to the PDK2 promoter after PDK2 gene silencing; IgG was used as a negative control. ns=not significant, \* $P < 0.05$ , \*\* $P < 0.01$ ; All data represent mean  $\pm$  SEM.

lengths into luciferase reporter plasmids, and then transfected the constructs into neurons that were then treated or not treated with 50  $\mu$ M CORT for 24 h. The results showed that pGL3-P1 (−2000 to 0 bp) and pGL3-P3 (−1000 to 0 bp) exhibited high levels of luciferase expression, whereas pGL3-P2 (−2000 to −1000 bp) did not affect luciferase activity (Fig. 3g). This indicated that the PDK2 promoter region between −1000 and 0 bp is critical for its expression in the CORT treatment. GR-binding sites in the PDK2 promoter region (from −997 to −983 bp and from −816 to −802 bp), which were predicted using the JASPAR database, were mutated (Fig. 3h) and cloned into the luciferase reporter plasmids, which were then transfected into neurons. Luciferase activity was determined for pGL3-P3, pGL31-mut1 (−997 to −983 bp), pGL3-mut2 (−816 to −802 bp), and pGL3-Basic (negative control [NC]) in cells treated or not treated with 50  $\mu$ M CORT. As shown in Fig. 3i, the luciferase activity of pGL3-P3 was 2- and 5-fold higher than that of pGL3-mut2 and pGL31-mut1, respectively, indicating that the promoter activity of PDK2 was more significantly inhibited by mutation in the −997 to −983 bp region than by mutation in the −816 to −802 bp region.

To verify the role of GR in the regulation of PDK2 promoter activity, we constructed a GR expression plasmid (pCDNA3.1-GR). Neurons expressing pCDNA3.1-GR showed significantly higher luciferase activity than those not expressing pCDNA3.1-GR (Fig. 3j), an effect that was dependent on GR concentration (Supplementary Fig. 8f). GR overexpression enhanced the PDK2 mRNA level (Supplementary Fig. 8g). Monitoring PDK2 promoter activity using GR-targeting siRNA and evaluating the efficiency of RNA interference (RNAi) by western blot analysis (Supplementary Fig. 8h, i) revealed a marked reduction in PDK2 promoter activity and PDK2 expression in si-GR-treated cells (Supplementary Fig. 8j, k). To further determine whether GR interacts with the PDK2 promoter, neurons were transfected with si-GR, treated or not treated with CORT, and then subjected to the ChIP assay. A DNA fragment of the predicted size was obtained using anti-GR antibody but not anti-IgG antibody (control). Moreover, the ChIP signal was strengthened in the CORT treatment, and weakened by GR silencing (Fig. 3k). Taken together, these findings suggest that GR binds to the PDK2 promoter and regulates PDK2 expression in neurons.

### Silencing PDK2 attenuates CORT-induced disturbance of the TCA cycle carbon flux

Mitochondrial membrane potential is the driving force for ATP synthesis, and is a crucial parameter for assessing mitochondrial function and metabolism [36]. To characterize the effect of PDK2 on mitochondrial function, the interference efficiency of siRNAs was validated at protein levels (Supplementary Fig. 9a). We next analyzed the  $\Delta\Psi_m$  by flow cytometry. Treatment with CORT led to a significant reduction in high  $\Delta\Psi_m$  in neurons at 24 h relative to that in neurons treated with NC siRNA (si-NC); however, this effect was significantly attenuated when PDK2 was silenced (Supplementary Fig. 9b). To assess mitochondrial function in response to PDK2 knockdown, the OCR (which reflects the cellular respiration capacity) of neurons was measured. We observed that CORT treatment led to a significant reduction in mitochondrial respiratory capacity (basal OCR, maximal OCR, and ATP-coupled

OCR) compared with the control; however, these effects were attenuated by PDK2 depletion (Fig. 4a–d). We traced carbon flux into the TCA cycle intermediates after PDK2 silencing. The  $^{13}\text{C}$ -labeled glucose can be metabolized into M+1 and M+3 pyruvate via glycolysis. Both M+1 and M+3 pyruvate enters the mitochondria, are converted into M+1 and M+2 acetyl-CoA by PDH, and then enter the TCA cycle (Fig. 4e and Supplementary Fig. 9c). The mass isotopologue distribution of citrate (from M+1 to M+6),  $\alpha$ -ketoglutarate (from M+1 to M+5), fumarate (from M+1 to M+4), and malate (from M+1 to M+4) decreased in the presence of CORT, while PDK2 silencing markedly alleviated this decrease (Fig. 4f–i). Total  $^{13}\text{C}$  enrichment was significantly decreased after the CORT treatment; however, the opposite was observed with PDK2 knockdown (Supplementary Fig. 9d–g). These results suggest that exposure to CORT inhibits carbon flux from the glycolysis pathway into the TCA cycle, leading to an insufficient supply of energy necessary for neuronal function. Conversely, PDK2 depletion exerts a significant promotive effect on glucose flux into the TCA cycle.

### PDK2 inhibition attenuates CSDS-induced depressive behaviors

Dichloroacetate (DCA), a PDK inhibitor, suppresses PDH phosphorylation and promotes pyruvate conversion to acetyl-CoA [37]. To assess whether the GR-PDK2-PDH axis affects the behavior of CSDS mice, the mice were treated with RU486 (20 mg/kg/day) or DCA (100 mg/kg/day) intraperitoneally once daily for 10 consecutive days in the CSDS treatment (Fig. 5a). We found that the daily injection of RU486 or DCA not only significantly ameliorated the SI ratio but also increased the number of stress-resilient mice (Fig. 5b). RU486 or DCA also rescued the CSDS-induced depression-like behaviors in SPT, FST and EPM (Fig. 5c–e). Additionally, CSDS increased PDK2 and p-PDH levels, and treatment with RU486 or DCA markedly reversed these effects (Fig. 5f). We also found that DCA or RU486 increased PDH activity, citric acid content, ATP level, and NADH/NAD<sup>+</sup> ratio (Fig. 5g–j). To further confirm the neuroprotective effect of DCA, potential morphological alterations occurring in cortical neurons were observed. Hematoxylin-eosin (HE) and Nissl staining results showed that morphological abnormalities were ameliorated in RU486- or DCA-treated neurons. As shown in Supplementary Fig. 10a–c, HE staining showed normal cell morphology in the control group, but abnormal cell morphology with nucleus pyknosis and disorderly arranged in the CSDS group. Nissl staining also revealed reduced Nissl bodies and accompanied with swelling, disorganized cells as well as membrane loss in the CSDS group. After treatment with RU486 or DCA, cell morphology was restored and the number of Nissl bodies was significantly increased. The number of neuronal apoptotic cells in the cortex was markedly higher in the CSDS group than in the CTRL group; however, this effect was reversed with RU486 or DCA treatment (Supplementary Fig. 10d, e).

### Neuronal-targeted PDK2 knockdown increases PDH activity and enhances the resilience to stress

To investigate the role of GR or PDK2 on PDH activity, selected GR or PDK2 shRNA sequences were embedded into an miR30

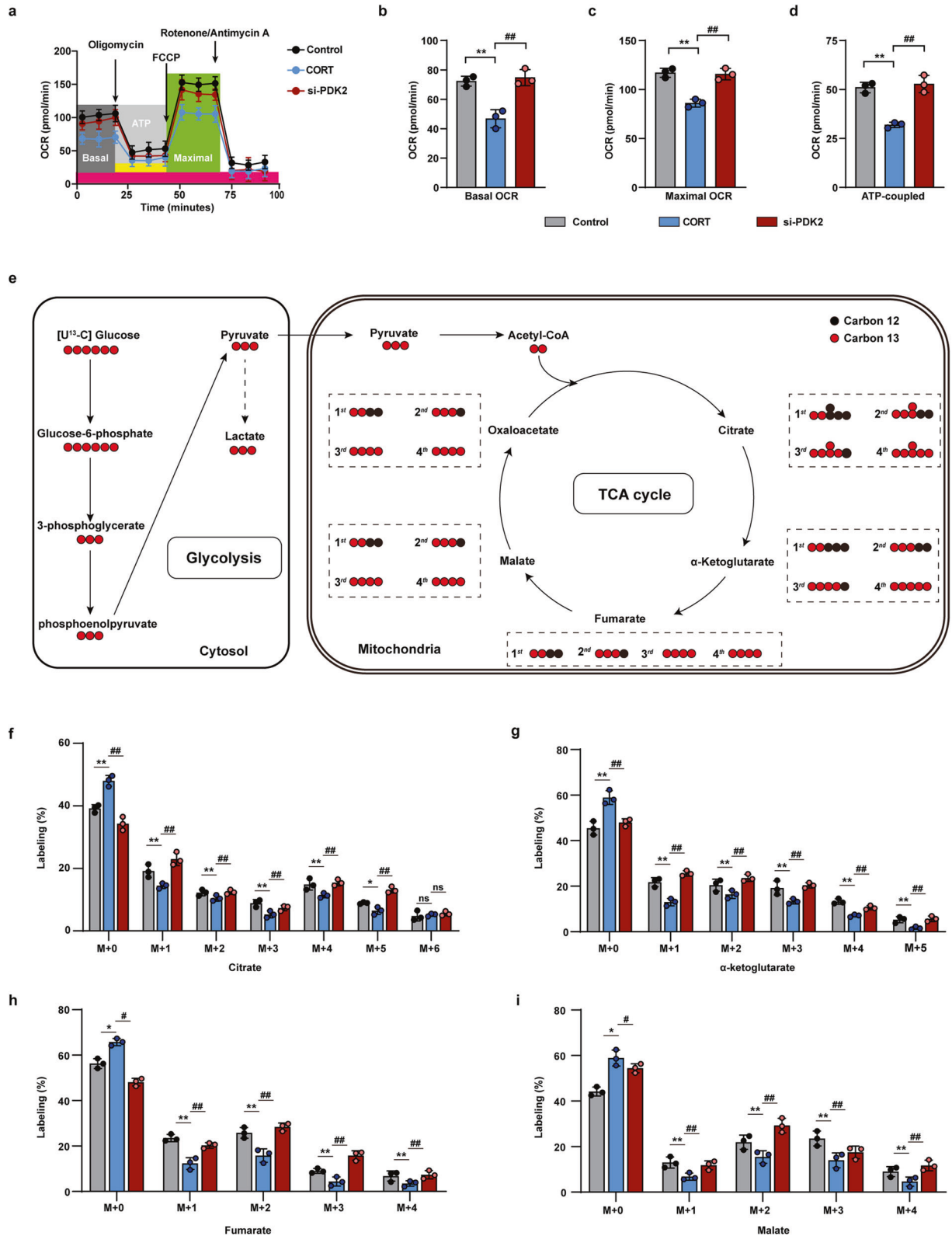
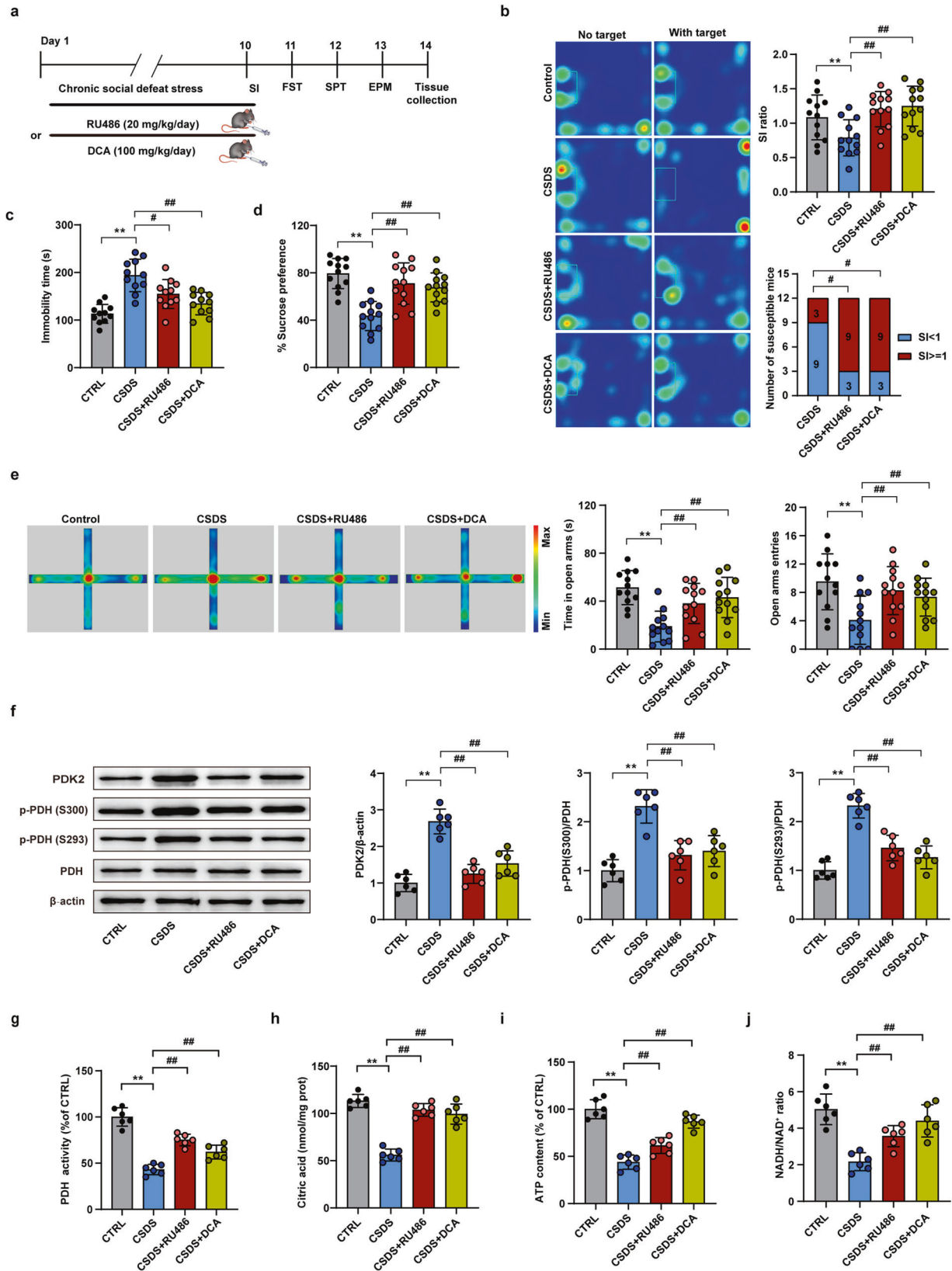


**Fig. 4 Silencing PDK2 regulates oxygen consumption rate and ameliorates CORT-induced disturbance of TCA cycle carbon flux.** **a** Measurement of OCR in PDK2-silenced primary cortical neurons cells using a Seahorse analyzer. **b–d** Graphical representations of the basic OCR, maximal OCR, and ATP-linked OCR after CORT treatment and si-PDK2 treatment.  $n = 3$ ; One-way ANOVA. **e** Schematic presentation <sup>13</sup>C-labeled from [U-<sup>13</sup>C]<sub>6</sub> glucose carbon atoms of first, second, third, and fourth turn in TCA cycling, respectively. The <sup>13</sup>C-labeled glucose can be metabolized into M+3 pyruvate via glycolysis. M+3 pyruvate enters the mitochondria and are converted into M+2 acetyl-CoA by PDH, which then enters the TCA cycle. Black and red circles illustrate unlabeled and <sup>13</sup>C-labeled carbon atoms, respectively. Comparisons of mass isotopologue distributions of citrate (**f**), α-ketoglutarate (**g**) fumarate (**h**) malate (**i**) in the TCA cycle.  $n = 3$ ; One-way ANOVA. \* $P < 0.05$ , \*\* $P < 0.01$ ; # $P < 0.05$ , ## $P < 0.01$ ; All data represent mean±SEM.



backbone. AAV-sh-NC, AAV-sh-GR, or AAV-sh-PDK2 were injected into the frontal cortex, and after three weeks, mice underwent 10 days of CSDS (Fig. 6a). First, we verified the efficiency of GR or PDK2 knockdown by AAV-mediated shRNA. Immunofluorescence

staining results showed the co-localization of EGFP and  $\beta$  III-tubulin positive cells (Supplementary Fig. 11a, b). As expected, GR or PDK2 expression was greatly reduced in cortex injected with the virus compared with the scramble shRNA group (Fig. 6b, c;

**Fig. 5 PDK inhibition attenuates CSDS-induced depressive behaviors.** **a** Experimental design of the CSDS procedure and intraperitoneal (i.p.) RU486 or DCA administration. **b** (Left) Heatmap of the trajectory of mice and (Right) SI ratio and statistics of the number of susceptible mice.  $n = 12$ ; One-way ANOVA. RU486 and DCA treatment reduced immobility time in the FST (**c**) and increased sucrose preference in the SPT (**d**).  $n = 12$ ; One-way ANOVA. **e** (Left) Heatmap of the trajectory of mice and (Right) RU486 and DCA treatment increased the time spent in the open arms and number of open arm entries of the EPM test.  $n = 12$ ; One-way ANOVA. **f** The effect of RU486 and DCA treatment on PDK2, phosphorylated PDH, and unphosphorylated PDH proteins levels in the cortex.  $n = 6$ ; One-way ANOVA. Effect of RU486 or DCA treatment on PDH activity (**g**), citric acid content (**h**), ATP level (**i**), and NADH/NAD<sup>+</sup> ratio (**j**).  $n = 6$ ; One-way ANOVA. \* $P < 0.05$ , \*\* $P < 0.01$ ; # $P < 0.05$ , ## $P < 0.01$ ; All data represent mean  $\pm$  SEM.

Supplementary Fig. 11c–e), indicating successful knockdown of GR or PDK2 genes. Previous literatures suggested that inhibition of GR activity may lead to early depressive-like episodes [38], whereas some studies have also demonstrated that inhibition of GR alone does not impact behavior of mice [18, 39, 40]. To test whether GR inhibition alone would cause depressive-like behavior, we assessed the possible behavioral changes in control mice (Supplementary Fig. 12a). We observed that mice injected with AAV-sh-GR showed no significant difference in the EPM (Supplementary Fig. 12b–d), SPT (Supplementary Fig. 12e) and FST (Supplementary Fig. 12f) compared to mice injected with AAV-sh-NC. In accordance, deletion of PDK2 also did not cause any behavioral changes (Supplementary Fig. 12b–f). We next examined whether GR-specific knockdown and PDK2-specific knockdown would increase resilience to stress. The results showed that CSDS mice with GR or PDK2 knockdown showed higher SI than the scramble shRNA (AAV9-hSyn-sh-NC) group, suggesting that GR or PDK2 prevents the induction of stress susceptibility (Fig. 6d). Mice injected with AAV9-hSyn-sh-GR and AAV9-hSyn-sh-PDK2 particles showed increased time spent on open arms and open arm entries in the elevated plus maze, increased sucrose preference in the SPT, and reduced immobility time in the FST (Supplementary Fig. 13a–d). In addition, GC–MS analysis revealed that the suppression of GR or PDK2 expression markedly decreased the level of lactate, while increasing the contents of citrate,  $\alpha$ -ketoglutarate, fumarate, and malate (Supplementary Fig. 13e). We next investigated the effect of GR or PDK2 knockdown on PDH activity and phosphorylation. As illustrated in Fig. 6e–g, GR knockdown significantly reduced the level of PDK2 mRNA and protein. Additionally, GR or PDK2 knockdown markedly decreased PDH phosphorylation at both Ser293 and Ser300 residues. Notably, GR or PDK2 suppression had no effect on PDH expression but increased PDH activity. Our results showed that ATP content and NADH/NAD<sup>+</sup> ratio were significantly higher in AAV9-hSyn-sh-GR- and AAV9-hSyn-sh-PDK2-injected mice than in the AAV9-hSyn-sh-NC-injected mice (Fig. 6h, i).

## DISCUSSION

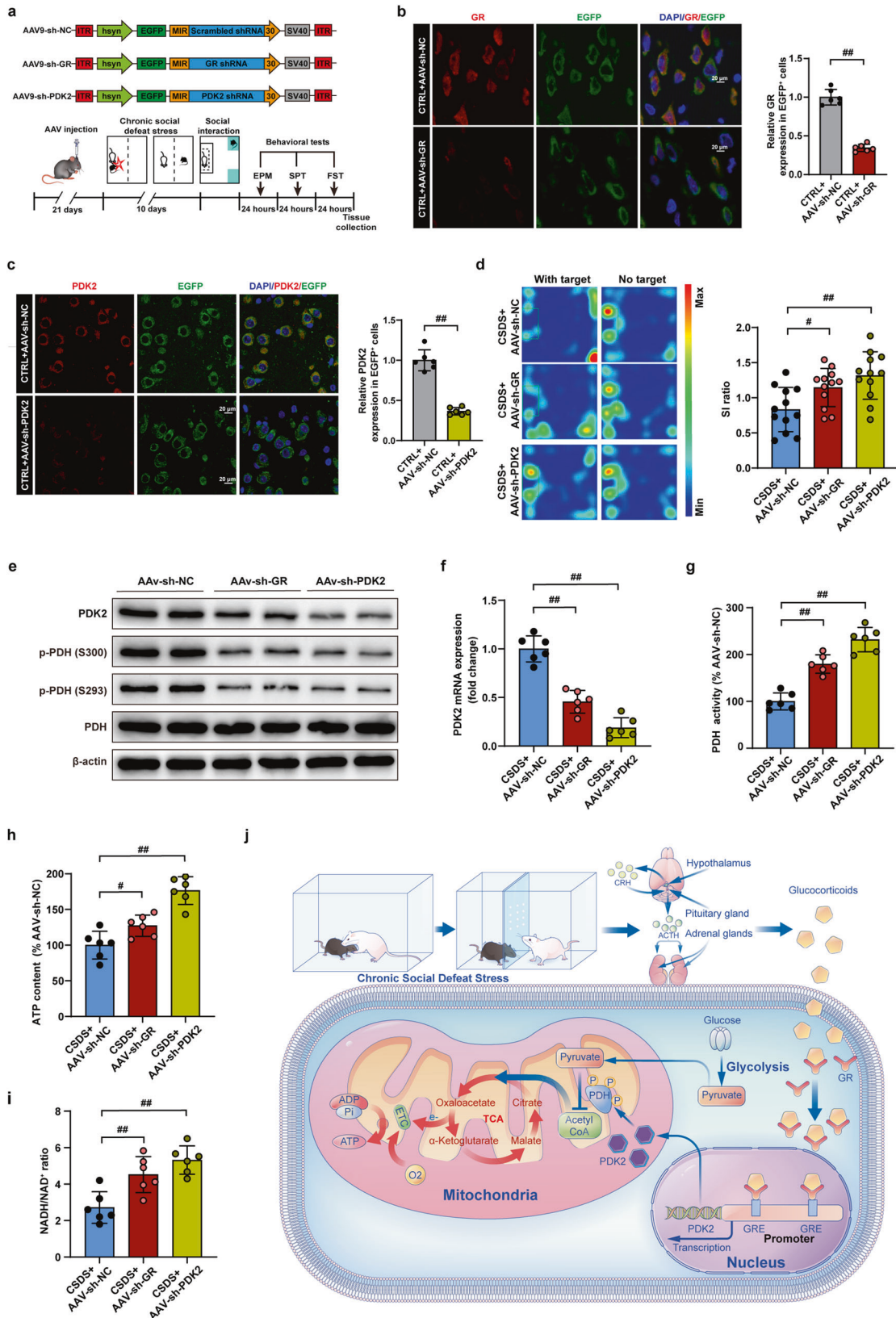
In the present study, we demonstrated that PDK2 plays a vital role in regulating brain energy metabolism and the pathogenesis of depression in the cortex. We showed that depression leads to an abnormal TCA cycle in both CSDS mice and MDD patients. PDK2 and p-PDH expression were upregulated in the frontal cortex of CSDS mice. We further found that, in neurons, the glucocorticoid-GR complex translocated into the nucleus and regulates PDK2 expression by directly binding to GREs in the PDK2 promoter region, leading to PDH phosphorylation and consequently reduced PDH enzymatic activity and decreased glucose flux into the TCA cycle (Fig. 6j). Inhibition of the GR or PDK2 significantly and effectively attenuated CSDS-induced social deficits and depression-like behavior.

Normal functioning of the brain requires a continuous supply of energy, and brain activation produces dynamic changes in energy requirements [41]. Glucose is the major energy source in the adult brain, and provides energy via glycolysis and the TCA cycle [42]. Accumulating evidence demonstrates that TCA cycle function is perturbed in many neurodegenerative disorders, including

Alzheimer's disease, Parkinson's disease, Huntington's disease, and amyotrophic lateral sclerosis [43]. Some metabolomics studies revealed that TCA cycle intermediates were down-regulated, indicating energy metabolism dysfunction may correlate with the occurrence of depression [44, 45]. One recent study also found a significant reduction in glycolysis in the hippocampus of rats with depression-like behavior, whereas the TCA cycle was impaired only in the frontal cortex [46]. Consistent with this, our study demonstrated that depression drives TCA cycle dysfunction as evidenced by the decrease in the contents of TCA cycle intermediates not only in the cortex of CSDS mice but also in the serum of both CSDS mice and MDD patients. Our results are consistent with those from studies reported by Wang et al. showing the decrease in serum levels of citric acid and  $\alpha$ -ketoglutarate in the animal model of depression [47]. Meanwhile, metabolomics analysis showed that the serum level of citric acid in patients with depression has also been decreased [48]. Our findings are also consistent with the previous study demonstrating that the levels of TCA cycle intermediates, such as malate and  $\alpha$ -ketoglutarate, are negatively correlated with Hamilton Depression Rating Scale scores [49]. These results strongly lend weight to the theory that depression is associated with the dysfunctional TCA cycle and energy metabolism in the brain.

The PDH complex plays a central role in regulating metabolic flux by linking glycolysis and the TCA cycle under physiological conditions [25, 50]. PDKs and PDP exert opposing modulatory effects on PDH activity. Specifically, phosphorylation inhibits, while dephosphorylation upregulates PDH activity [28, 51]. Given that PDKs are widely expressed in the brain [52], the present study examined PDK expression and PDH enzymatic activity in different brain regions. We found increased PDK2 expression and decreased PDH activity in the cortex and hippocampus. However, there was no correlation between PDH activity and SI ratios in hippocampus. We also found that while the PDK2 expression was significantly increased in hypothalamus and amygdala, there was no detectable difference in PDH activity. Although the most striking impact of CSDS on PDK2-PDH axis was observed in the cortex and it has been reported that PDK2 is mostly abundant in the cortical region [53], the effect of altered PDK2 in other brain regions should be noted. A recent study demonstrated that inhibition of hippocampal PDK2 reduced oxidative stress after pilocarpine-induced seizures [54]. Additionally, another study found that PDK2 plays crucial role in hypothalamic inflammation and consequent impairment of feeding behavior in streptozotocin-induced diabetic mice [55]. These findings suggest that PDK2 may have distinct roles in different brain regions. Therefore, the functions of PDK2 in other brain regions should be further investigated.

PDK2 is a nuclear gene encoding a mitochondrial protein responsible for regulating phosphorylation of PDH. In line with our results, Rahman et al. found that PDK2 is negligibly expressed in microglia, but is expressed in neurons and astrocytes, and plays a role in regulating neuroinflammation in astrocytes [55]. Our data from primary cell culture also confirmed the *in vivo* findings and showed that PDK2 was expressed in both neurons and astrocytes, which is consistent with previous research showing the highly expressed PDK2 in both cell types [56]. Under CSDS, PDK2 expression was markedly induced in neurons, slightly but significantly upregulated in astrocytes, and still hardly detectable in microglia. In general, the energy requirements of astrocytes are



predominantly dependent on glycolysis, whereas neurons exhibit higher unphosphorylated PDH levels, faster TCA cycle activity, and greater dependence on oxidative phosphorylation than astrocytes [57, 58]. Therefore, astrocytes possess a greater metabolic plasticity

compared to neurons, i.e., they can better adapt their energy metabolism in response to mitochondrial stress [59], and CSCS-induced alterations in PDK2 expression may render neurons teetering on the brink of energy failure more susceptible to

**Fig. 6 GR-specific or PDK2-specific knockdown in neurons increases PDH activity and blocks CSDS-induced depressive behaviors.** **a** Schematic of the AAV9-hSyn-sh-NC, AAV9-hSyn-sh-GR, and AAV9-hSyn-sh-PDK2 constructs, and experimental timeline of viral infection. Verification of GR (**b**) and PDK2 (**c**) knockdown efficiency in the cortex by immunofluorescence. **d** Effect of AAV9-mediated knockout of GR or PDK2 on SI ratio; (Left) Heatmap of the trajectory of mice and (Right) statistical graph of SI ratio.  $n = 12$ ; One-way ANOVA. **e** Effect of AAV9-mediated knockout of GR or PDK2 on PDK2, phosphorylated PDH, and unphosphorylated PDH protein levels in the cortex. Effect of AAV9-mediated knockout of GR or PDK2 on PDK2 mRNA level (**f**), PDH activity (**g**), ATP level (**h**), and NADH/NAD<sup>+</sup> ratio (**i**) in the cortex.  $n = 6$ ; One-way ANOVA. **j** Schematic diagram showing how glucocorticoid regulates PDK2 expression, impairing brain energy metabolism. CSDS activates the HPA axis, leading to the release of GCs from the adrenal cortex. GCs enter the brain through the blood-brain barrier, where they bind to the GR. The GCs-GR complex enters the neuronal nucleus, and binds to GREs in the PDK2 promoter to regulate PDK2 expression, leading to the phosphorylation of PDH, the consequent decrease in PDH enzymatic activity and glucose flux into the TCA cycle, and further regulation of brain energy metabolism. <sup>#</sup> $P < 0.05$ , <sup>##</sup> $P < 0.01$ ; All data represent mean  $\pm$  SEM.

fluctuations in energy supply due to the high energy demands. This finding further strengthened the importance of the PDK2-PDH axis in the regulation of energy homeostasis in the neuron to face sustained stress [60].

In response to stress, the adrenal gland generally secretes large amounts of GCs, which can impair cognitive function by directly acting on different brain regions [19, 61]. Our results are consistent with those of previous studies, which showed that chronic stress leads to elevated levels of CORT (in rodents) and cortisol (in patients with depression) [21, 62, 63]. Functionally relevant GR gene polymorphisms have been linked to increased susceptibility to depression [64]. In addition, we found that CORT induced the nuclear translocation of GR in neurons and elicited an increase in PDK2 content. Consistent with the results of our in vitro analysis, using GR-specific antagonist or knockdown of GR inhibited PDK2 expression and blocked PDH phosphorylation, and thereby increased PDH activity. Once inside the cells, GCs bind to the GR and then translocate into the nucleus from the cytoplasm, where they bind to GREs and regulate the expression of target genes [65, 66]. Our data also suggested that high PDK2 expression was likely due to the specific binding of the GR to GREs in the promoter region of PDK2 in neurons. To test this possibility, we performed transcription factor binding site prediction using the JASPAR database, constructed luciferase reporter plasmids containing either wild-type or mutated PDK2 promoter sequences, and performed GR overexpression analysis. We found that mutating either of the two predicted GR-binding sites resulted in the partial reduction of luciferase activity, indicating that both sites are important for GR binding. The effect of GR overexpression and knockdown on luciferase activity was examined in neurons. As expected, luciferase activity gradually increased in a GR concentration-dependent manner, whereas GR knockdown resulted in decreased luciferase activity. In addition, ChIP-PCR assay results confirmed that the GR binds to the PDK2 promoter. Previously, studies have focused only on GR binding sites in the PDK4 promoter region. GREs were identified between -824 and -809 bp of the PDK4 promoter as well as more than 6000 bp upstream of the transcriptional start site of the same gene [67, 68].

Neuroimaging studies have also indicated that impaired cerebral energy metabolism is a common feature in patients with depression [69]. Neurons have extremely high energy demand that mainly relies on ATP production in mitochondria [70]. Here, we demonstrated that ATP content was decreased in the cortex and hippocampus of CSDS mice. Stable isotope labeling showed that exposure to CORT blocked carbon flux into the TCA cycle, while PDK2 silencing elicited the opposite effect. Additionally, CORT administration was found to impair mitochondrial respiration and diminish ATP production in neurons, with marked changes in basic OCR, ATP-linked OCR, and maximal OCR; however, silencing PDK2 using siRNA ameliorated this effect. Many previous studies have reported that RU486 or DCA can easily penetrate the blood-brain barrier, and play an important protective role in the brain [71-74]. Here, we found that the administration of DCA particularly reduced PDK2 expression and PDH phosphorylation, enhanced PDH activity, and further conferred neuroprotection. Likewise, the GR antagonist,

RU486, also restored the CSDS-induced disturbance of PDK2. Nevertheless, considering the non-specific effects of DCA on PDK activity, we constructed AAV vectors to knockout PDK2 or GR in the cortex, which are under control hSyn neuron-specific promoter. We also found that the neuron-specific knockdown of GR or PDK2 increased PDH activity, improved TCA cycle dysfunction, increased ATP level, and alleviated CSDS-induced depression-like behavior. These results were consistent with the effects of pharmacological inhibitors, suggesting GR signaling interacts with the PDK-PDH axis to promote the stress-induced neurological dysfunction.

In summary, our data confirmed that GR activate the transcription of PDK2 by directly binding to its promoter region and by regulating neuronal TCA flux and ATP production, which may play an important role in maintaining brain energy homeostasis. Additionally, our study showed that the inhibition of PDK2 expression improved CSDS-induced behavioral deficits and brain injury. Our study identified a novel mechanism underlying the pathogenesis of depression, and provides a potential therapeutic target for the treatment of this condition.

## REFERENCES

- Gururajan A, Reif A, Cryan JF, Slattery DA. The future of rodent models in depression research. *Nat Rev Neurosci*. 2019;20:686-701.
- Kendler KS, Karkowski LM, Prescott CA. Causal relationship between stressful life events and the onset of major depression. *Am J Psychiatry*. 1999;156:837-41.
- Chen X, Luo J, Leng Y, Yang Y, Zweifel LS, Palmiter RD, et al. Ablation of type III adenylyl cyclase in mice causes reduced neuronal activity, altered sleep pattern, and depression-like phenotypes. *Biol Psychiatry*. 2016;80:836-48.
- Liu F, Shi J, Tanimukai H, Gu J, Gu J, Grundke-Iqbal I, et al. Reduced O-GlcNAcylation links lower brain glucose metabolism and tau pathology in Alzheimer's disease. *Brain*. 2009;132:1820-32.
- Attwell D, Laughlin S. An energy budget for signaling in the grey matter of the brain. *J Cereb Blood Flow Metab*. 2001;21:1133-45.
- Kolar D, Kleteckova L, Brozka H, Vales K. Brain energy metabolism and its role in animal models of depression, bipolar disorder, schizophrenia and autism. *Neurosci Lett*. 2021;760:136003.
- Martin SA, Souder DC, Miller KN, Clark JP, Sagar AK, Eliceiri KW, et al. GSK3 $\beta$  Regulates Brain Energy Metabolism. *Cell Rep*. 2018;23:1922-31.e1924.
- A O, U M, L F, A GC. Energy metabolism in childhood neurodevelopmental disorders. *EBioMedicine*. 2021;69:103474.
- Goyal MS, Vlassenko AG, Blazey TM, Su Y, Couture LE, Durbin TJ, et al. Loss of brain aerobic glycolysis in normal human aging. *Cell Metab*. 2017;26:353-60.e353.
- Fang W, Xiao N, Zeng G, Bi D, Dai X, Mi X, et al. APOE4 genotype exacerbates the depression-like behavior of mice during aging through ATP decline. *Translational Psychiatry*. 2021;11:507.
- Wu J, Zhao Y, Park YK, Lee JY, Gao L, Zhao J, et al. Loss of PDK4 switches the hepatic NF- $\kappa$ B/TNF pathway from pro-survival to pro-apoptosis. *Hepatology*. 2018;68:1111-24.
- Ryall JG, Cliff T, Dalton S, Sartorelli V. Metabolic Reprogramming of Stem Cell Epigenetics. *Cell Stem Cell*. 2015;17:651-62.
- Lindqvist D, Wolkowitz O, Picard M, Ohlsson L, Bersani F, Fernström J, et al. Circulating cell-free mitochondrial DNA, but not leukocyte mitochondrial DNA copy number, is elevated in major depressive disorder. *Neuropsychopharmacol*. 2018;43:1557-64.
- Andreazza AC, Shao L, Wang JF, Young LT. Mitochondrial complex I activity and oxidative damage to mitochondrial proteins in the prefrontal cortex of patients with bipolar disorder. *Arch Gen Psychia*. 2010;67:360-8.

15. Okamoto N, Viswanatha R, Bittar R, Li Z, Haga-Yamanaka S, Perrimon N, et al. A membrane transporter is required for steroid hormone uptake in drosophila. *Dev Cell*. 2018;47:294–305.e297.
16. Vyas S, Maatouk L. Contribution of glucocorticoids and glucocorticoid receptors to the regulation of neurodegenerative processes. *CNS Neurol Disord Drug Targets*. 2013;12:1175–93.
17. Pariante CM. Why are depressed patients inflamed? A reflection on 20 years of research on depression, glucocorticoid resistance and inflammation. *Eur Neuropsychopharm*. 2017;27:554–9.
18. Solomon MB, Wulsin AC, Rice T, Wick D, Myers B, McKlveen J, et al. The selective glucocorticoid receptor antagonist CORT 108297 decreases neuroendocrine stress responses and immobility in the forced swim test. *Horm Behav*. 2014;65:363–71.
19. Wei Q, Fentress HM, Hoversten MT, Zhang L, Hebda-Bauer EK, Watson SJ, et al. Early-life forebrain glucocorticoid receptor overexpression increases anxiety behavior and cocaine sensitization. *Biol Psychiatry*. 2012;71:224–31.
20. Keller J, Gomez R, Williams G, Lembke A, Lazzaroni L, Murphy GM, et al. HPA axis in major depression: cortisol, clinical symptomatology and genetic variation predict cognition. *Mol Psychiatry*. 2017;22:527–36.
21. Paugh SW, Bonten EJ, Savic D, Ramsey LB, Thierfelder WE, Gurung P, et al. NALP3 inflammasome upregulation and CASP1 cleavage of the glucocorticoid receptor cause glucocorticoid resistance in leukemia cells. *Nat Genet*. 2015;47:607–14.
22. Roqueta-Rivera M, Esquejo RM, Phelan PE, Sandor K, Daniel B, Foufelle F, et al. SETDB2 links glucocorticoid to lipid metabolism through insig2a regulation. *Cell Metab*. 2016;24:474–84.
23. Magomedova L, Cummins CL. Glucocorticoids and metabolic control. *Handb Exp Pharmacol*. 2016;233:73–93.
24. Yau JL, Seckl JR. Local amplification of glucocorticoids in the aging brain and impaired spatial memory. *Front Aging Neurosci*. 2012;4:24.
25. Park S, Jeon JH, Min BK, Ha CM, Thoudam T, Park BY, et al. Role of the pyruvate dehydrogenase complex in metabolic remodeling: differential pyruvate dehydrogenase complex functions in metabolism. *Diabetes Metab J*. 2018;42:270–81.
26. Wang G, Liu X, Xie J, Meng J, Ni X. PDK-1 mediated Hippo-YAP-IRS2 signaling pathway and involved in the apoptosis of non-small cell lung cancer cells. *Biosci Rep*. 2019;39:BSR20182099.
27. Bowker-Kinley MM, Davis WI, Wu P, Harris RA, Popov KM. Evidence for existence of tissue-specific regulation of the mammalian pyruvate dehydrogenase complex. *Biochem J*. 1998;329:191–6.
28. Jeong JY, Jeoung NH, Park KG, Lee IK. Transcriptional regulation of pyruvate dehydrogenase kinase. *Diabetes Metab J*. 2012;36:328–35.
29. Faron-Górecka A, Kuśmider M, Kolasa M, Żurawek D, Szafran-Pilch K, Gruca P, et al. Chronic mild stress alters the somatostatin receptors in the rat brain. *Psychopharmacology*. 2016;233:255–66.
30. Jiang C, Lin WJ, Sadahiro M, Labonté B, Menard C, Pfau ML, et al. VGF function in depression and antidepressant efficacy. *Mol Psychiatry*. 2018;23:1632–42.
31. Montagud-Romero S, Blanco-Gandía MC, Reguilón MD, Ferrer-Pérez C, Ballestin R, Miñarro J, et al. Social defeat stress: Mechanisms underlying the increase in rewarding effects of drugs of abuse. *Eur J Neurosci*. 2018;48:2948–70.
32. Zou WJ, Song YL, Wu MY, Chen XT, You QL, Yang Q, et al. A discrete serotonergic circuit regulates vulnerability to social stress. *Nat Commun*. 2020;11:4218.
33. Carlson D, David LK, Gallagher NM, Vu MT, Shirley M, Hultman R, et al. Dynamically timed stimulation of corticolimbic circuitry activates a stress-compensatory pathway. *Biol Psychiatry*. 2017;82:904–13.
34. Poolman TM, Farrow SN, Matthews L, Loudon AS, Ray DW. Pin1 promotes GR transactivation by enhancing recruitment to target genes. *Nucl Acids Res*. 2013;41:8515–25.
35. Vaz-Silva J, Gomes P, Jin Q, Zhu M, Zhuravleva V, Quintremil S, et al. Endolysosomal degradation of Tau and its role in glucocorticoid-driven hippocampal malfunction. *EMBO J*. 2018;37:e99084.
36. Hoefs SJ, Dieteren CE, Distelmaier F, Janssen RJ, Epplen A, Swarts HG, et al. NDUFA2 complex I mutation leads to Leigh disease. *Am J Hum Genet*. 2008;82:1306–15.
37. Liao EC, Hsu YT, Chuah QY, Lee YJ, Hu JY, et al. Radiation induces senescence and a bystander effect through metabolic alterations. *Cell Death Dis*. 2014;5:e1255.
38. Han YM, Kim MS, Jo J, Shin D, Kwon SH, Seo JB, et al. Decoding the temporal nature of brain GR activity in the NFκB signal transition leading to depressive-like behavior. *Mol Psychiatry*. 2021;26:5087–96.
39. Nasca C, Bigio B, Zelli D, Nicoletti F, McEwen BS. Mind the gap: glucocorticoids modulate hippocampal glutamate tone underlying individual differences in stress susceptibility. *Mol Psychiatry*. 2015;20:755–63.
40. Schmidt MV, Sterlemann V, Wagner K, Niederleitner B, Ganea K, Liebl C, et al. Postnatal glucocorticoid excess due to pituitary glucocorticoid receptor deficiency: differential short- and long-term consequences. *Endocrinology*. 2009;150:2709–16.
41. Diaz-García CM, Mongeon R, Lahmann C, Koveal D, Zucker H, Yellen G. Neuronal stimulation triggers neuronal glycolysis and not lactate uptake. *Cell Metab*. 2017;26:361–74.e364.
42. Zheng H, Yu WM, Shen J, Kang S, Hambardzumyan D, Li JY, et al. Mitochondrial oxidation of the carbohydrate fuel is required for neural precursor/stem cell function and postnatal cerebellar development. *Sci Adv*. 2018;4:eaat2681.
43. Zacharias NM, Chan HR, Sailasuta N, Ross BD, Bhattacharya P. Real-time molecular imaging of tricarboxylic acid cycle metabolism in vivo by hyperpolarized 1-(13C) diethyl succinate. *J Am Chem Soc*. 2012;134:934–43.
44. Shao WH, Chen JJ, Fan SH, Lei Y, Xu HB, Zhou J, et al. Combined metabolomics and proteomics analysis of major depression in an animal model: perturbed energy metabolism in the chronic mild stressed rat cerebellum. *Omic*. 2015;19:383–92.
45. Chen JJ, Xie J, Li WW, Bai SJ, Wang W, Zheng P, et al. Age-specific urinary metabolite signatures and functions in patients with major depressive disorder. *Aging*. 2019;11:6626–37.
46. Głombik K, Detka J, Kurek A, Budziszewska B. Impaired brain energy metabolism: involvement in depression and hypothyroidism. *Front Neurosci*. 2020;14:586939.
47. Bu Q, Zhang LK, Guo X, Feng Y, Yan H, Cheng W, et al. The antidepressant effects and serum metabolomics of bifid triple viable capsule in a rat model of chronic unpredictable mild stress. *Front Nutr*. 2022;9:947697.
48. Shen D, Zhao H, Gao S, Li Y, Cheng Q, Bi C, et al. Clinical serum metabolomics study on fluoxetine hydrochloride for depression. *Neurosci Lett*. 2021;746:135585.
49. Kaddurah-Daouk R, Bogdanov MB, Wikoff WR, Zhu H, Boyle SH, Churchill E, et al. Pharmacometabolomic mapping of early biochemical changes induced by sertraline and placebo. *Transl Psychiat*. 2013;3:e223.
50. Sullivan CR, O'Donovan SM, McCullumsmith RE, Ramsey A. Defects in bioenergetic coupling in schizophrenia. *Biol Psychiatry*. 2018;83:739–50.
51. Ni M, Solmonson A, Pan C, Yang C, Li D, Notzon A, et al. Functional assessment of lipoyltransferase-1 deficiency in cells, mice, and humans. *Cell Rep*. 2019;27:1376–86.e1376.
52. Jha MK, Jeon S, Suk K. Pyruvate dehydrogenase kinases in the nervous system: their principal functions in neuronal-glia metabolic interaction and neuro-metabolic disorders. *Curr Neuropharmacol*. 2012;10:393–403.
53. Nakai N, Obayashi M, Nagasaki M, Sato Y, Fujitsuka N, Yoshimura A, et al. The abundance of mRNAs for pyruvate dehydrogenase kinase isoenzymes in brain regions of young and aged rats. *Life Sci*. 2000;68:497–503.
54. Lee SH, Choi BY, Kho AR, Hong DK, Kang BS, Park MK, et al. Combined Treatment of dichloroacetic acid and pyruvate increased neuronal survival after seizure. *Nutrients*. 2022;14:4804.
55. Rahman MH, Bhusal A, Kim JH, Jha MK, Song GJ, Go Y, et al. Astrocytic pyruvate dehydrogenase kinase-2 is involved in hypothalamic inflammation in mouse models of diabetes. *Nat Commun*. 2020;11:5906.
56. Halim ND, Mcfate T, Mohyeldin A, Okagaki P, Korotchkina LG, Patel MS, et al. Phosphorylation status of pyruvate dehydrogenase distinguishes metabolic phenotypes of cultured rat brain astrocytes and neurons. *Glia*. 2010;58:1168–76.
57. Castelli V, Benedetti E, Antonosante A, Catanesi M, Pitari G, Ippoliti R, et al. Neuronal cells rearrangement during aging and neurodegenerative disease: metabolism, oxidative stress and organelles dynamic. *Front Mol Neurosci*. 2019;12:132.
58. Cunnane SC, Trushina E, Morland C, Prigione A, Casadesus G, Andrews ZB, et al. Brain energy rescue: an emerging therapeutic concept for neurodegenerative disorders of ageing. *Nat Rev Drug Discov*. 2020;19:609–33.
59. Bolaños JP. Bioenergetics and redox adaptations of astrocytes to neuronal activity. *J Neurochem*. 2016;139:115–25.
60. Zeisel A, Muñoz-Manchado AB, Codeluppi S, Lönnerberg P, La Manno G, Juréus A, et al. Brain structure. Cell types in the mouse cortex and hippocampus revealed by single-cell RNA-seq. *Science*. 2015;347:1138–42.
61. Holsboer F, Ising M. Stress hormone regulation: biological role and translation into therapy. *Annu Rev Psychol*. 2010;61:81.
62. Kim CS, Brager DH, Johnston D. Perisomatic changes in h-channels regulate depressive behaviors following chronic unpredictable stress. *Mol Psychiatry*. 2018;23:892–903.
63. Iyo AH, Feyissa AM, Chandran A, Austin MC, Regunathan S, Karolewicz B. Chronic corticosterone administration down-regulates metabotropic glutamate receptor 5 protein expression in the rat hippocampus. *Neuroscience*. 2010;169:1567–74.
64. van Rossum EF, Binder EB, Majer M, Koper JW, Ising M, Modell S, et al. Polymorphisms of the glucocorticoid receptor gene and major depression. *Biol Psychiatry*. 2006;59:681–8.
65. Johnson TA, Chereji RV, Stavreva DA, Morris SA, Hager GL, Clark DJ. Conventional and pioneer modes of glucocorticoid receptor interaction with enhancer chromatin in vivo. *Nucl Acids Res*. 2018;46:203–14.
66. Magomedova L, Tiefenbach J, Zilberman E, Le Billan F, Voisin V, Saikali M, et al. ARG11 is a transcriptional coactivator and splicing regulator important for stress hormone signaling and development. *Nucl Acids Res*. 2019;47:2856–70.
67. Kwon HS, Huang B, Unterman TG, Harris RA. Protein kinase B-α inhibits human pyruvate dehydrogenase kinase-4 gene induction by dexamethasone through inactivation of FOXO transcription factors. *Diabetes*. 2004;53:899–910.

68. Connaughton S, Chowdhury F, Attia RR, Song S, Zhang Y, Elam MB, et al. Regulation of pyruvate dehydrogenase kinase isoform 4 (PDK4) gene expression by glucocorticoids and insulin. *Mol Cell Endocrinol.* 2010;315:159–67.
69. Xu Z, Guo X, Yang Y, Tucker D, Lu Y, Xin N, et al. Low-level laser irradiation improves depression-like behaviors in mice. *Mol Neurobiol.* 2017;54:4551–9.
70. Moffat C, Pacheco JG, Sharp S, Samson AJ, Bolland KA, Huang J, et al. Chronic exposure to neonicotinoids increases neuronal vulnerability to mitochondrial dysfunction in the bumblebee (*Bombus terrestris*). *Faseb J.* 2015;29:2112–9.
71. Zhu X, Huang Y, Li S, Ge N, Li T, Wang Y, et al. Glucocorticoids reverse diluted hyponatremia through inhibiting arginine vasopressin pathway in heart failure rats. *J Am Heart Assoc.* 2020;9:e014950.
72. Perry R, Wang Y, Cline GW, Rabin-Court A, Song J, Dufour S, et al. Leptin mediates a glucose-fatty acid cycle to maintain glucose homeostasis in starvation. *Cell.* 2018;172:234–48.e217.
73. Abemayor E, Kovachich GB, Haugaard N. Effects of dichloroacetate on brain pyruvate dehydrogenase. *J Neurochem.* 1984;42:38–42.
74. Check JH, Wilson C, Cohen R, Sarumi M. Evidence that mifepristone, a progesterone receptor antagonist, can cross the blood brain barrier and provide palliative benefits for glioblastoma multiforme grade IV. *Anticancer Res.* 2014;34:2385–8.

### ACKNOWLEDGEMENTS

We thank all volunteers, patients, and their families for their contribution in this study.

### AUTHOR CONTRIBUTIONS

CW and CC wrote the manuscript. PX and LZ performed the in vitro experiments. CW, CC and HX conducted the in vivo experiments. BC and PJ conducted data analysis. PJ contributed to study conception and edited the manuscript.

### FUNDING

This study was supported by the National Natural Science Foundation of China (No. 81602846; No. 82272253), Natural Science Foundation of Shandong Province (No. ZR2021MH145), Taishan Scholar Project of Shandong Province (No. tsqn201812159), China International Medical Foundation (No. Z-2018-35-2002), Research Fund for Lin He's Academician Workstation of New Medicine and Clinical Translation of Jining Medical University (No. JYHL2021FMS19), and Key Research and Development Projects of Jining City (No. 2021YXNS084).

### COMPETING INTERESTS

The authors declare no competing interests.

### ADDITIONAL INFORMATION

**Supplementary information** The online version contains supplementary material available at <https://doi.org/10.1038/s41380-023-02098-9>.

**Correspondence** and requests for materials should be addressed to Pei Jiang.

**Reprints and permission information** is available at <http://www.nature.com/reprints>

**Publisher's note** Springer Nature remains neutral with regard to jurisdictional claims in published maps and institutional affiliations.

Springer Nature or its licensor (e.g. a society or other partner) holds exclusive rights to this article under a publishing agreement with the author(s) or other rightsholder(s); author self-archiving of the accepted manuscript version of this article is solely governed by the terms of such publishing agreement and applicable law.